First Measurement of the Nuclear Charge Radii of Short-Lived Lithium Isotopes

Wilfried Nörtershäuser, Andreas Dax*, Guido Ewald, Stefan Götte, Reinhard Kirchner, H.-Jürgen Kluge, Thomas Kühl, Rodolfo Sanchez and Agnieszka Wojtaszek†
Gesellschaft für Schwerionenforschung, D-64291 Darmstadt, Germany

Bruce A. Bushaw
Pacific Northwest National Laboratory, P.O. Box 999, Richland, WA 99352, USA

Gordon W. F. Drake
Department of Physics, University of Windsor, Windsor, Ontario, Canada, N9B 3P4

Zong-Chao Yan
Department of Physics, University of New Brunswick, Fredericton, New Brunswick, Canada E3B 5A3

Claus Zimmermann
Eberhard Karls Universität Tübingen, Physikalisches Institut, D-72076 Tübingen, Germany

December 22, 2004

Abstract. A novel method for the determination of nuclear charge radii of lithium isotopes is presented. Precise laser spectroscopic measurements of the isotope shift in the lithium $2s \rightarrow 3s$ transition are combined with highly accurate atomic physics calculation of the mass dependent isotope shift to extract the charge-distribution-sensitive information. This approach has been used to determine the charge radii of ^{8,9}Li for the first time.

Keywords: nuclear charge radius, laser spectroscopy, isotope shift, halo nucleus

1. Introduction

Nuclear properties of lithium isotopes have attracted much interest over the last decades. Particularly the discovery of the huge matter radius of ^{11}Li by Tanihata et al. [1] triggered many investigations on that nucleus and the picture of a two-neutron halo was established. Today, this is still a very active field, *e.g.* the two-neutron separation energy [2] and the spectroscopic nuclear quadrupole moment [3] have been re-measured recently with improved accuracy, and new data on the ^{11}Li decay suggests that β decay can occur inside the ^{9}Li core and

* current address: CERN, CH-1211 Geneva 23, Switzerland
† current address: Faculty of Physics, Warsaw University PL-00-681, Poland

one of the two halo-neutrons can survive in a halo-like configuration [4]. A very interesting topic for nuclear structure theory is the interaction between the halo-neutrons and the protons inside the core. It is still an open question, whether the additional neutrons influence the proton distribution inside the ^{9}Li core. It could be solved by measuring the nuclear charge radii of ^{9}Li and ^{11}Li.

Root-means square (rms) charge radii of short-lived isotopes are usually extracted from isotope shift measurements [5, 6]. To isolate the charge radius information, the mass-dependent part of the isotope shift has to be separated from the field shift contribution. For heavy nuclei the mass effect is very small and can often be neglected, while for light nuclei the situation is reversed: The mass shift is dominant and the field shift is only on the order of 10^{-4} of the total isotope shift. Moreover, the mass shift in many-electron systems cannot be calculated easily since all electron correlations must be taken into account. Until recently, such accurate calculations were only possible for helium and helium-like systems. These results allowed a precise laser-spectroscopic determination of the ^{3}He charge radius [7] and are the foundation for a determination of the charge radius of the two-neutron halo nucleus ^{6}He [8]. A few years ago, Yan and Drake [9] succeeded in extending those calculations to three-electron systems and published results for the mass-dependent isotope shift of all lithium isotopes. These are accurate enough to allow a determination of charge radii to an accuracy of a few percent, provided that the isotope shift can be measured to a relative uncertainty of better than 10^{-5}. Such an accuracy cannot be obtained using collinear fast beam spectroscopy, one of the workhorses for isotope shift measurements on unstable isotopes. Here, the precision is limited by the knowledge of the exact beam energy and typical uncertainties for isotope shifts are on the order of 1 MHz, which is as large as the expected field shift between ^{6}Li and ^{11}Li. The desired accuracy can only be reached by a Doppler-free measurement on thermal lithium atoms or by laser spectroscopy on cooled lithium atoms or ions inside an atom or ion trap. We have chosen the former and performed laser spectroscopy on the $2s \rightarrow 3s$ two-photon transition for ^{6,7,8,9}Li at the on-line mass separator at GSI Darmstadt, Germany. We report on those measurements and discuss the results, which can be used to discriminate between different nuclear models.

2. Theory

The isotope shift (IS) in an electronic transition can be divided into the mass shift (MS) and the field shift (FS)

$$\delta\nu_{\rm IS}^{AA'} = \delta\nu_{\rm MS}^{AA'} + \delta\nu_{\rm FS}^{AA'} \ . \tag{1}$$

The field shift in the transition is caused by the modification of the Coulomb potential that the electrons experience while they are inside the nucleus. For light isotopes, the wave function of the electron can be assumed to be constant over the nuclear volume and the field shift can be expressed as

$$\delta\nu_{\rm FS}^{AA'} = -\frac{2\pi}{3} Ze^2 \Delta|\psi_e(0)|^2 \delta\langle r_c^2\rangle^{AA'} = F_i \delta\langle r_c^2\rangle^{AA'} \ , \tag{2}$$

where $\Delta|\psi_e(0)|^2$ is the change of the electron charge density at the nucleus between the lower and the upper state of the transition and $\delta\left\langle r_c^2\right\rangle^{AA'}$ is the change in the mean-square nuclear charge radii between the isotopes A and A'. Provided that the mass shift $\delta\nu_{\rm MS}^{AA'}$ and the electronic part F_i can be calculated to sufficient accuracy the change in the charge radius can be easily obtained according to

$$\delta\langle r_c^2\rangle^{AA'} = \frac{\delta\nu_{\rm IS}^{AA'} - \delta\nu_{\rm MS}^{AA'}}{F_i} \ . \tag{3}$$

The starting point for accurate mass-shift calculations is the solution of the non-relativistic Schrödinger equation including the mass polarization operator, using variational calculations in Hylleraas coordinates. The derived wave functions are then used to calculate relativistic and QED corrections. Finite nuclear mass effects are taken into account up to second order by perturbation theory. Theoretical results for the mass shift of all lithium isotopes were first published in [9] and have since been improved by including QED recoil corrections [10] and a new approach to calculating the Bethe Logarithm [11]. The most recent values are listed in Tab. I. The constant F_i for the $2s \rightarrow 3s$ transition was calculated to be -1.5661 MHz/fm^2. The uncertainty in the mass shift values is mainly limited by the accuracy of the relativistic recoil term.

3. Laser Excitation Scheme

Figure 1(A) shows the excitation and ionization scheme used. Two-photon excitation from the $2s$ ground state to the $3s$ state (2×735 nm)

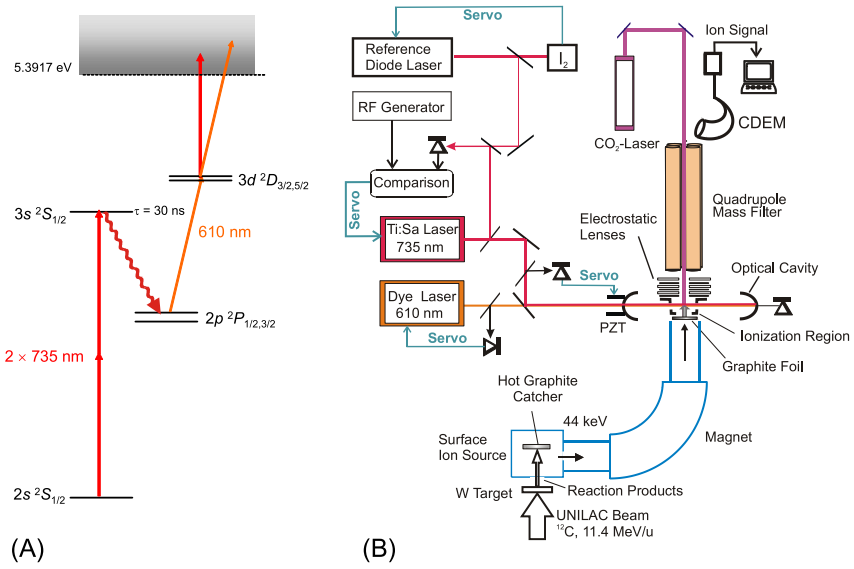

Figure 1. Excitation scheme (A) and experimental setup (B) for the resonance ionization of lithium.

is followed by resonance ionization. Ionization directly out of the $3s$ level can be attained with laser light of wavelength $\lambda < 614$ nm but is not very efficient, while resonant coupling of the $3s$ state to another, higher-lying state leads to prohibitively large AC-Stark shifts and broadening. Thus, precise spectroscopy in the $2s \rightarrow 3s$ transition must be decoupled from the efficient resonance ionization. This is achieved by including the $3s \rightarrow 2p$ spontaneous decay in the excitation scheme. Out of the $2p$ state the atoms are resonantly excited to the $3d$ state (610 nm) and then non-resonantly ionized by absorption of either a 735 nm or a 610 nm photon. Both, two-photon transition and the ionization step require high laser intensities. Therefore, both laser beams are coupled into an enhancement cavity which is built around the interaction region. This has the additional advantage that the $2p \rightarrow 3d$ transition is strongly power-broadened and a precise tuning of the 610 nm light to one of the fine structure transitions is not necessary. Rather, the $3d$ fine structure levels will overlap and provide an increased ionization efficiency. With this excitation scheme we have measured overall efficiencies exceeding 10^{-4}, which is sufficient for measurements on ^{11}Li with production yields on the order of only 10^4/s.

4. Experimental Method

The experimental setup is shown schematically in Fig. 1(B). The short-lived isotopes are produced by an 11.4 MeV/u ^{12}C beam impinging onto a graphite or a tungsten target for ^{8}Li and ^{9}Li, respectively. The reaction products are surface ionized, accelerated to 44 keV and mass separated in a 60° sector magnet. Typical yields of approximately 200,000 and 150,000 ions/s are obtained for ^{8}Li and ^{9}Li, respectively. The ions are then stopped inside a thin graphite foil (catcher) which is heated with a CO_2 laser to $\sim 2000°$C. The neutralized particles diffuse out of the foil and drift into the ionization region of a quadrupole mass filter (QMS). When they cross the laser beams they are resonantly ionized, the ions are extracted with the ion optics of the QMS, mass separated and detected with a channeltron-type detector. The laser system is shown in the left part of Fig. 1(B). A diode laser stabilized to the a_1 component of the I_2 $X\,^1\Sigma_g^+ \rightarrow B\,O_u^+$ $R(114)11-2$ hyperfine line using frequency modulation saturation spectroscopy provides a reference frequency relative to which the lithium resonance frequencies are measured. A titanium:sapphire (Ti:Sa) laser is used to produce the 735-nm light for the two-photon transition and a dye laser operated with Rhodamine 6G generates the 610-nm light for the $2p \rightarrow 3d$ transition. The Ti:Sa is stabilized relative to the reference laser using frequency-offset locking. The beat frequency between the reference laser and the Ti:Sa is counted with an RF counter and provides an accurate frequency axis for the resonance signals. The cavity is locked to the stabilized Ti:Sa laser via the Pound-Drever-Hall method while the dye laser is locked to a longitudinal mode of the cavity that is close to the resonance frequency of the $2p \rightarrow 3d$ transition. The resonators free-spectral range of $\sim$ 500 MHz and the strong saturation broadening ensures that a locking point within the flat top of the transition profile can always be found. More details of the experimental setup and the laser system can be found in [12, 13].

5. Results and Discussion

To observe the resonance signals, the Ti:Sa frequency is scanned across the two-photon resonances for the different isotopes and the count rate at the detector is recorded. For isotope-shift determinations, the observed resonance profiles are fitted with a line profile consisting of a Voigt profile for the narrow two-photon component and a broad underlying Gaussian profile caused by absorption of two photons from the same direction. A spectrum of ^{9}Li is shown in Fig. 2(A). Selection

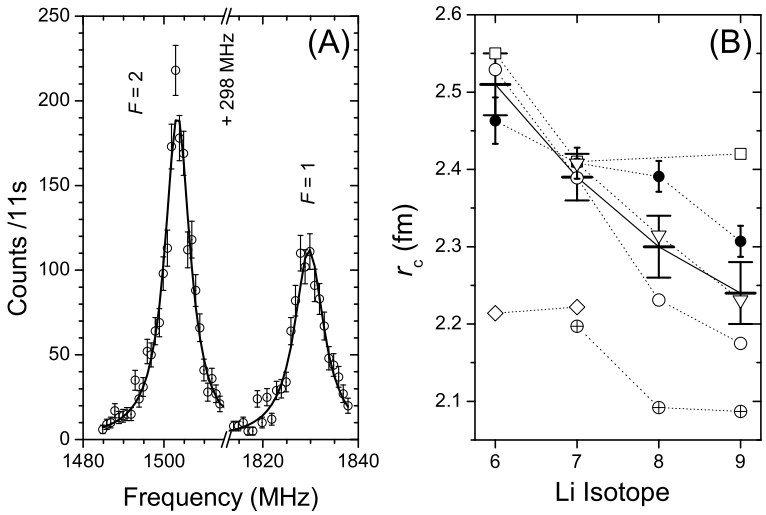

Figure 2. (A) Resonance profile of the $2s \rightarrow 3s$ two-photon transition for ^{9}Li. (B) The rms charge radii for ^{6,7,8,9}Li: (—) this measurement with $r_c(^7\mathrm{Li})$ from electron scattering as reference; (●) obtained from interaction cross section measurements using Glauber theory [25]; (⊕) LBSM [19]; (◊) NCSM [20]; (∇) SVMC [21]; (□) DCM [22]; (○) GFMC calculations using AV18/IL2 potentials [23, 24].

rules for a $^2S_{1/2} \rightarrow {}^2S_{1/2}$ two-photon transition dictate that $\Delta F = 0$. Thus, only two well-separated hyperfine components are observed. In the region between the two peaks the laser frequency has been quickly tuned without data acquisition. The symbols indicate the experimental data points and the solid line shows the fitted resonance profile. The fitted center frequencies of the hyperfine components are combined to obtain the center of gravity. This value is then corrected for residual AC Stark shifts and used to calculate the change in the mean-square charge radius $\delta\langle r_c^2\rangle^{7,A}$ relative to ^{7}Li according to Eq. 3. To obtain absolute charge radii, we took the ^{7}Li rms charge radius of 2.39(3) fm measured by electron scattering [14] as a reference. The results are listed in Tab. I and shown in Fig. 2(B) together with predictions from different theories. The point-proton radii r_p, given in most theoretical work, have been converted to charge radii r_c by folding in the proton and neutron mean square charge radii according to

$$r_c = \sqrt{\langle r_p^2\rangle + \langle R_p^2\rangle + (N/Z)\langle R_n^2\rangle}\ , \qquad (4)$$

where $\langle R_p^2 \rangle^{1/2} = 0.895(18)$ fm [15] is the rms charge radius of the proton, $\langle R_n^2 \rangle = -0.116(5)$ fm^2 [16] is the rms charge radius of the neutron, and N and Z are the neutron and proton numbers, respectively. Note that in [13] we have used the proton radius of $\left\langle R_p^2 \right\rangle^{1/2} = 0.862$ fm [17] for the conversion. This leads to a change of about 0.01 fm for all isotopes. Five different theoretical approaches are shown in the figure: large-basis shell-model (LBSM) [19], *ab-initio* no-core shell model (NCSM) [20], stochastic variational multi-cluster (SVMC) [21], dynamic correlation model (DCM) [22] and Greens function Monte Carlo (GFMC) [23, 24] calculations. Best agreement with the experimental values is observed for the SVMC approach. GFMC calculations were carried out using a variety of effective low-energy model potentials for the two- and three-nucleon interactions. Shown are the results for the combination of the AV18 two-body with the IL2 three-body potential, because those give the best agreement with the experiment. On the other hand, the DCM, LBSM and the NSCM calculations do not agree with our results. For comparison, the figure includes model-dependent r_c values derived from experimental interaction cross sections using Glauber-type calculations [25]. These results show a similar trend of decreasing charge radii, but to a slightly smaller extent.

The reported results demonstrate that this method is able to determine nuclear charge radii of lithium isotopes to an accuracy of a few percent, even with production yields as small as 150,000 ions/s. The goal is now the measurement of the isotope shift between ^{9}Li and ^{11}Li at the ISAC mass separator at TRIUMF (Vancouver, Canada) to determine the change in the nuclear charge radius of the ^{9}Li core when the two neutrons are added.

Acknowledgements

This work is supported from BMBF contract No. 06TU203. Support from the U.S. DOE under contract No. DE-AC06-76RLO 1830 (B.B.), NSERC and SHARCnet.(G.W.F.D. and Z.-C.Y.) is acknowledged. A.W. was supported by a Marie-Curie Fellowship of the European Community Programme IHP under contract number HPMT-CT-2000-00197.

References

1. I. Tanihata, H. Hamagaki, O. Hashimoto, Y. Shida, N. Yoshikawa, K. Sugimoto, O. Yamakawa, T. Kobayashi, and N. Takahashi, Phys. Rev. Lett. **55**, (1985) 2676-2679.

Table I. Isotope shift of the $2\,^2S_{1/2} \rightarrow 3\,^2S_{1/2}$ transition and extracted $\delta\langle r_c^2\rangle^{A,7}$ and rms charge radii r_c.

	IS, MHz	MS, MHz	$\delta\langle r_c^2\rangle^{A,7}$, fm^2	r_c, fm	Reference
^{6}Li	-11 453.95(13)	-11453.01(6)	0.60(11)	2.51(4)	This work.
	-11 453.734(30)		0.47(5)	2.49(4)	[18]
			0.79(25)	2.55(4)	[14]
^{7}Li		0		2.39(3)	[14]
^{8}Li	8 635.79(15)	8635.11 (4)	-0.43(11)	2.30(4)	This work.
^{9}Li	15 333.14(18)	15332.02(8)	-0.72(14)	2.24(4)	This work.
^{11}Li		25102.13(17)†			

† This value was calculated using a ^{11}Li mass of 11.043796(29) amu [26]. Recently, it has been remeasured with higher accuracy [2], but the final value has not been published yet.

2. C. Bachelet, G. Audi, C. Gaulard, C. Guénaut, F. Herfurth, D. Lunney, M. De Saint Simon, C. Thibault, and the ISOLDE Collaboration, to be published.
3. G. Neyens *et al.*, to be published.
4. F. Sarazin, J.S. Al-Khalili, G.C. Ball, G. Hackman, P.M. Walker, R.A.E. Austin, B. Eshpeter, P. Finlay, P.E. Garrett, G.F. Grinyer, K.A. Koopmans, W.D. Kulp, J.R. Leslie, D. Melconian, C.J. Osborne, M.A. Schumaker, H.C. Scraggs, J. Schwarzenberg, M.B. Smith, C.E. Svensson, J.C. Waddington, and J.L. Wood, Phys. Rev. C **70**, (2004) 031302-5.
5. E.W. Otten, in *Treatise on heavy-ion science* **8**, edited by D.A. Bromley, (Plenum Press, New York, 1989) 517.
6. H.-J. Kluge and W. Nörtershäuser, Spectrochim. Acta Part B **58**, (2003) 1031-1045.
7. D. Shiner, R. Dixson, and V. Vedantham, Phys. Rev. Lett. **74**, (1995) 3553-3556.
8. L.-B. Wang, P. Mueller, K. Bailey, G.W.F. Drake, J.P. Greene, D. Henderson, R.J. Holt, R.V.F. Janssens, C.L. Jiang, Z.-T. Lu, T.P. O'Connor, R.C. Pardo, K.E. Rehm, J.P. Schiffer, and X.D. Tang, Phys. Rev. Lett. **93**, (2004) 142501.
9. Z.-C. Yan and G.W.F. Drake, Phys. Rev. A **61**, (2000) 022504.
10. Z.-C. Yan and G.W.F. Drake, Phys. Rev. A **66**, (2002) 042504.
11. Z.-C. Yan and G.W.F. Drake, Phys. Rev. Lett. **91**, (2003) 113004.
12. W. Nörtershäuser, A. Dax, G. Ewald, I. Katayama, R. Kirchner, H.-J. Kluge, T. Kühl, R. Sanchez, I. Tanihata, M. Tomaselli, H. Wang, and C. Zimmermann, Nucl. Instrum. Meth. Phys. Res. B **204**, (2003) 644-648.
13. G. Ewald, W. Nörtershäuser, A. Dax, S. Götte, R. Kirchner, H.-J. Kluge, T. Kühl, R. Sanchez, A. Wojtaszek, B.A. Bushaw, G.W.F. Drake, Z.-C. Yan, and C. Zimmermann, Phys. Rev. Lett. **93**, (2004) 113002; Phys. Rev. Lett. **94**, (2005) 039901.
14. C.W. de Jager, H. deVries, and C. deVries, At. Data Nucl. Data Tables **14**, (1974) 479-508.
15. I. Sick, Phys. Lett. B **576**, (2003) 62-67.

16. S. Kopecky, J.A. Harvey, N.W. Hill, M. Krenn, M. Pernicka, P. Riehs, and S. Steiner, Phys. Rev. C **56**, (1997) 2229-2237.
17. G.G. Simon et al. G.G. Simon, C. Schmitt, F. Borkowski, and V.H. Walther, Nucl. Phys. A **333**, (1980) 381-391.
18. B.A. Bushaw, W. Nörtershäuser, G. Ewald, A. Dax and G.W.F. Drake, Phys. Rev. Lett. **91**, (2003) 043004.
19. P. Navrátil and B.R. Barrett, Phys. Rev. C **57**, (1998) 3119-3128.
20. P. Navrátil, and W.E. Ormand, Phys. Rev. C, **68**, (2003) 034305.
21. Y. Suzuki, R.G. Lovas and K. Varga, Prog. Theor. Phys. Suppl. **146**, (2002) 413-421.
22. M. Tomaselli, T. Kühl, W. Nörtershäuser, G. Ewald, R. Sanchez, S. Fritzsche and S.G. Karshenboim, Can. J. Phys. **80**, (2002) 1347-1354.
23. S.C. Pieper and R.B. Wiringa, Annual Rev. Nucl. Part. Science **51**, (2001) 53-90.
24. S.C. Pieper, K. Varga and R.B. Wiringa, Phys. Rev. C **66**, (2002) 044310.
25. I. Tanihata, T. Kobayashi, O. Yamakawa, S. Shimoura, K. Ekuni, K. Sugimoto, N. Takahashi, T. Shimoda, and H. Sato, Phys. Lett. B **206**, (1988) 592-596.
26. G. Audi and A.H. Wapstra, Nucl. Phys. A **595**, (1995) 409-480.